Venting and Gas Generation from 18650 Lithium-ion Batteries with LFP Cathode Chemistry During Thermal Runaway

Christopher A. Almodovar, Lorenz R. Boeck, C. Regis L. Bauwens
Research Division, FM Global
Norwood, MA, USA

1 Introduction

The use of lithium-ion batteries (LIB) for energy storage applications is rapidly increasing in both residential and industrial settings. These systems can present new fire and explosion hazards, however, as LIBs have the potential to undergo thermal runaway (TR) – an uncontrolled rise in temperature due to runaway internal chemical reactions that can release significant quantities of flammable gases [1]. These energy storage systems are typically composed of an array of battery modules that each contain an array of unit cells, such as the 18650 form-factor cylindrical cell. When a single cell undergoes TR, adjacent cells and modules are at risk of entering TR due to heat transfer from the initiating cell. Predicting the propagation of TR through modules and systems, and the resulting release of flammable gas, requires a detailed understanding of the TR dynamics of individual cells, including thermal and electrochemical effects, the gas venting process, and heat transfer between cells. Furthermore, ignition of the released flammable gases may enhance the heat transfer to adjacent cells and, thus, have a significant effect on TR propagation, reaffirming the importance of understanding the venting process – from the gas's composition and its flammability limits to elevated heat release if ignition occurs.

This work is part of an ongoing effort to develop more advanced models for the hazard posed by LIB systems as well as improved techniques for explosion prevention and mitigation. To that end, an experimental apparatus was created to provide a consistent method to force 18650 form-factor LIBs into TR via thermal abuse under constant heating rates in a controlled environment. Previous works in other apparatuses, such as accelerating rate calorimeters, typically provide low heating rates of < 5 °C/min. Experimental analysis has revealed, however, that heating rates as high as several hundred °C/min can occur during cell-to-cell TR propagation [2]. The present work examines the effect of heating rate to identify its impact on cell venting, TR, and related gas generation. Additionally, this setup allows for measurements of characteristic temperatures and the amount of gas released, as well as the collection of vent gases for quantitative composition analysis and further reactivity testing.

Initial data of characteristic temperatures and the amount of gas generated are presented here for the TR of 18650 form-factor LIBs with lithium iron phosphate ($LiFePO_4$ or LFP) cathodes and carbon anodes. The gas release from 18650 cells occurs in two phases: the first occurs when the internal cell pressure exceeds the burst pressure of the safety vent and the second occurs during the rapid onset of TR. An analysis of venting and gas generation is performed by applying a venting model to estimate

Correspondence to: christopher.almodovar@fmglobal.com

the internal LIB cell pressure. These results provide insight into the internal state of the battery and will be used for future experiment design and model development for gas release from individual cells.

2 Experimental setup

Figure 1 shows a 3-D rendering of the experimental setup. The heater and LIB assembly were clamped inside a 20-L spherical vessel made of stainless steel that can maintain elevated or vacuum pressures. Feedthrough ports with electrical and TC (thermocouple) leads provided electrical power to the heater and temperature measurements of the gas in the enclosed volume and on the LIB surface. Internal pressure was measured with piezoresistive pressure transducers (Omega PX409 Series) with ranges of 350 kPa and 35 kPa and a bandwidth of 1 kHz. Prior to each experiment, two purge-vacuum cycles were performed with nitrogen before a final evacuation to about 800 Pa. Experiments were conducted at initial vacuum to produce undiluted gas samples that can be used for further reactivity testing. At present, the vessel's walls are not heated, but heating may be introduced in future work.

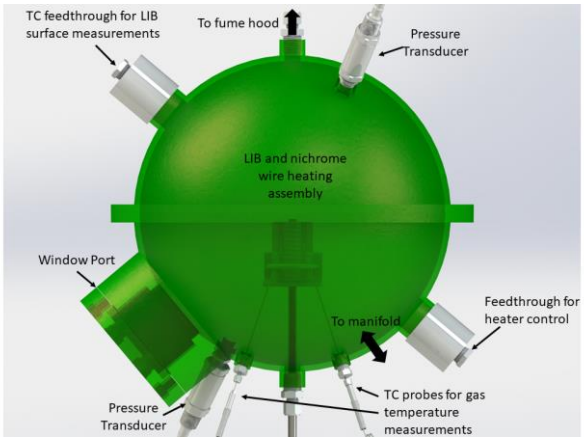

Figure 1: 3-D rendering of the experimental setup.

In this study, LFP batteries with 18650 form-factor and manufactured by K2-Energy were examined. A C7400 C-series battery analyzer was used to determine the state-of-health (SOH) and set the state-of-charge (SOC) for each LFP LIB cell to 100% prior to each experiment. At least one type-K TC was spot welded onto the LIB shell to measure surface temperature and control the heating rate.

The heater was made of coiled 26 AWG nichrome 80 wire sandwiched between two layers of Cotronics ceramic paper and held in place with a wrapping of fiberglass electrical tape with a silicone adhesive. The nichrome wire heater has a measured resistance of 3.7 Ohms. Power to the heater was supplied by a 24 V DC power supply (Acopian A24H1200), and the output of the power supply was controlled by pulse-width modulation (PWM). A PID controller was used to maintain a constant heating rate until TR. Heater voltage and current were also measured to determine the heating power.

Transient measurements from a typical experiment are shown in Figure 2. The top panel shows the heater power determined through measurements of current and voltage. The instantaneous power is not resolved in the figure's time scales since the power is being modulated by the PID-PWM signal, so the time-averaged power signal is more representative of the heater's power output. The right axis of the top panel shows TC signals measuring the surface temperature of the LIB. The bottom panel of Figure 2 shows the measured pressure of the 20-L spherical vessel and TC measurements of the gas volume. There are two regions distinguished by rapid pressure changes. The first rise occurs during the rupture of the safety vent and is referred to as initial venting. The second pressure rise occurs during TR and corresponds to a rapid rise in temperature of the LIB.

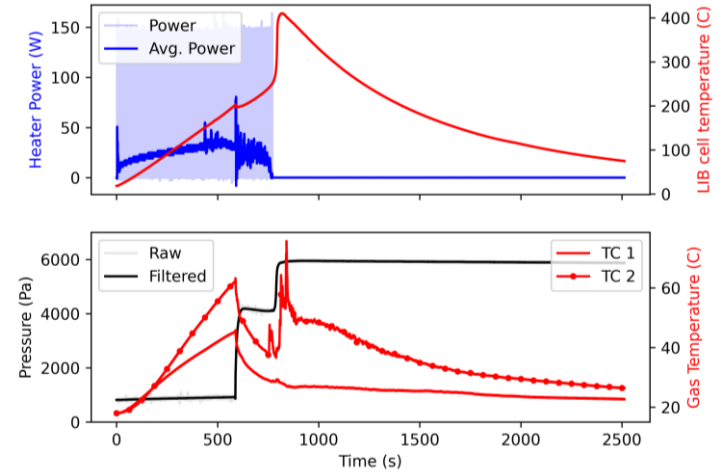

Figure 2: Representative measurements for an LIB TR experiment with a 20 °C/min heating rate under evacuated conditions.

3 Venting model

Previous works incorporated venting models to improve predictions of TR dynamics [3] and empirically studied the flow behavior of vent caps for 18650 form factor LIBs [4]. Here, those concepts are used to infer the internal pressure and venting flow regimes from experimental data of LIBs in TR. The initial venting of 18650 form factor LIBs is controlled by the rupture of the safety vent. Austin Mier et al. described the choked flow venting regime [4] of the initial blowdown. Using the perfect gas relations, Equation (1) describes the choked mass flow rate through a nozzle:

$$\dot{m} = C_d A^* \frac{P_0}{\sqrt{R_s T_0}} \sqrt{\gamma} \left(1 + \frac{\gamma - 1}{2}\right)^{-\frac{\gamma+1}{2(\gamma-1)}}, \tag{1}$$

where C_d is the discharge coefficient, A^* is the sonic area, P_0 is the total pressure of the flow, T_0 is the total temperature, R_s is the specific gas constant, and γ is the ratio of specific heats for the vented gas. In this form, the mass flow rate is proportional to the internal pressure in the LIB cell. Assuming constant γ and uniform cell temperature, the internal cell pressure can be estimated as a function of time from the mass flow rate inferred from the 20-L enclosure pressure evolution. The choked condition is only applicable under the following criterion:

$$P_\mathrm{crit} = P_\mathrm{e} \left(\frac{2}{\gamma + 1}\right)^{\frac{\gamma}{1-\gamma}} \leq P_0, \tag{2}$$

where P_e is the external pressure relative to the LIB (i.e., pressure in the 20-L sphere) and P_crit is the critical internal pressure that must be maintained to achieve choked flow. Otherwise, the mass flow rate must be reformulated for subsonic flow. Equation (3) is derived from the ideal gas relations for subsonic flow exiting a vessel [5]

$$\dot{m} = C_\mathrm{d} A \rho_0 \left(\frac{P_\mathrm{e}}{P_0}\right)^{\frac{1}{\gamma}} \sqrt{\frac{2\gamma}{\gamma - 1} \frac{P_0}{\rho_0} \left[1 - \left(\frac{P_\mathrm{e}}{P_0}\right)^{\frac{\gamma-1}{\gamma}}\right]}. \tag{3}$$

Here, ρ_0 is the density of the gas and is used here for brevity, but from the ideal gas law it can be written as $\rho_0 = P_0/R_s T_0$. Values used in this work for the discharge coefficient, C_d, and outlet area, A, of the nozzle are based on those reported by Austin Mier et al. [4] for two different vent caps. Their

methodology determined that despite different designs and geometries, the actual effective opening areas were similar in value with averages between 7 and 9 mm^2. Therefore, a value of 8 mm^2 was used in the model. The sonic area was also assumed to be equal to the subsonic exit area. The discharge coefficient was reported to vary with stagnation pressure and ranged from 0.75 to 0.95. A fixed value of 0.85 was used for C_d in the present model. The head space volume available in the LIB is estimated at 20% of the 16.5-cm^3 cell volume [6].

4 Results

The results of twenty experiments are summarized in Figure 3 where characteristic temperatures (a) and measured moles of gas released from the LIB (b) are plotted against average heating rates varied from approximately 10 to 80 °C/min. Figure 3(a) shows three characteristic temperatures. The temperature at venting (T_{vent}) is defined here as the temperature when the pressure derivative is 25% of its peak during the initial venting event. The temperature at the onset of TR (T_{onset}) is defined as the temperature where a line tangent to the temperature profile at the peak temperature derivative intersects with a projection of the imposed heating rate prior to TR. Finally, T_{max} is the maximum temperature measured during the TR event. The PID heater controller reduces the heating input once dT/dt exceeds the heating rate set point, so the sharp rise in temperature is due to internal heat generation. As a result, T_{max} occurs after external heating applied to the LIB has stopped. The measured characteristic temperatures generally increased with heating rate. Linear regression was performed on each of the characteristic temperatures versus prescribed heating rate. If one considers a null hypothesis of slope equaling zero, the alternative hypothesis for a non-zero slope returns p-values $\leq 10^{-6}$ for each fit, indicating that the slope is non-zero with a high level of significance.

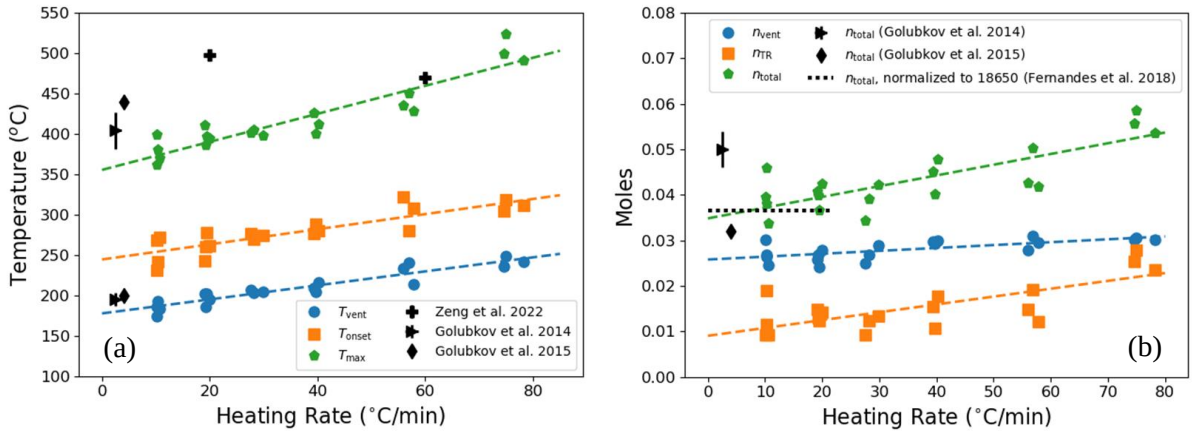

Figure 3: The effect of heating rate on characteristic temperatures (a) and moles (b) released during different stages of TR.

Figure 3(b) shows the moles released during the initial venting (n_{vent}), during thermal runaway (n_{TR}), and the sum of the two (n_{total}). In all experiments, $n_{vent} > n_{tr}$, with n_{vent}/n_{total} ranging from 0.52 to 0.77. At higher heating rates, the distinction between venting and TR is less pronounced. As a result, the initial venting process may not be complete before gas generation due to TR begins, but despite the potential overlap of events, n_{tr} was determined consistently. Linear regression was performed on n_{vent}, n_{TR}, and n_{total} versus the prescribed heating rate. For the n_{vent} regression, the p-value and R^2 value are 0.001 and 0.457, respectively. Thus, although the values span only 5.7 mmol, there is a statistically significant increase in n_{vent} with heating rate. There is a stronger correlation between the heating rate and n_{TR} (p-value = 0.0002, R^2 = 0.548), so preliminary results indicate that the increase in n_{total} is primarily dependent on the heating rate through the correlation with n_{TR}.

A deeper evaluation of the dynamics of the vent gas production can be made with the model presented

in Section 3. The number of moles released can be calculated from measured pressure, volume, and gas temperature, and the mass released can be determined using the vented mixture's molar mass. However, the instantaneous composition of the vented gas is unknown without quantitative transient gas analysis and the flow through the vents is likely a multiphase mixture of gaseous products from decomposition reactions and the battery electrolyte itself. To address the uncertainty of the exiting gas's composition, the model is evaluated at different mixture molar masses and specific heat ratios of the vented gas corresponding to two limiting cases of 1) a mixture of light molecules informed from LFP vent gas mixtures reported in the literature [7] [8] and 2) a mixture of heavy molecules corresponding to the electrolyte composition of LFP LIB cells reported by Golubkov et al [6]. Mixtures 1) and 2) have molar masses and specific heat ratios of 27.5 and 1.32 and 93.48 and 1.1, respectively. Using these mixture properties in the venting model provides reasonable bounds under the simplifying assumption that all vented mass is in a gaseous state.

Figure 4 shows pressure measurements and inferred parameters of an experiment with a 20 °C/min heating rate. The figure is separated into two regions: the first is the initial venting after rupture of the safety vent (565 – 585 s), and the second is venting during the onset of TR (880 – 900 s). The model presented in Section 3 is used to infer the internal pressure from the measurement of moles generated for each limiting mixture (gas or electrolyte) creating an uncertainty range of estimated LIB internal pressures. In addition, literature values for vent cap burst pressures and the envelope of critical pressure (see Equation (2)) are shown.

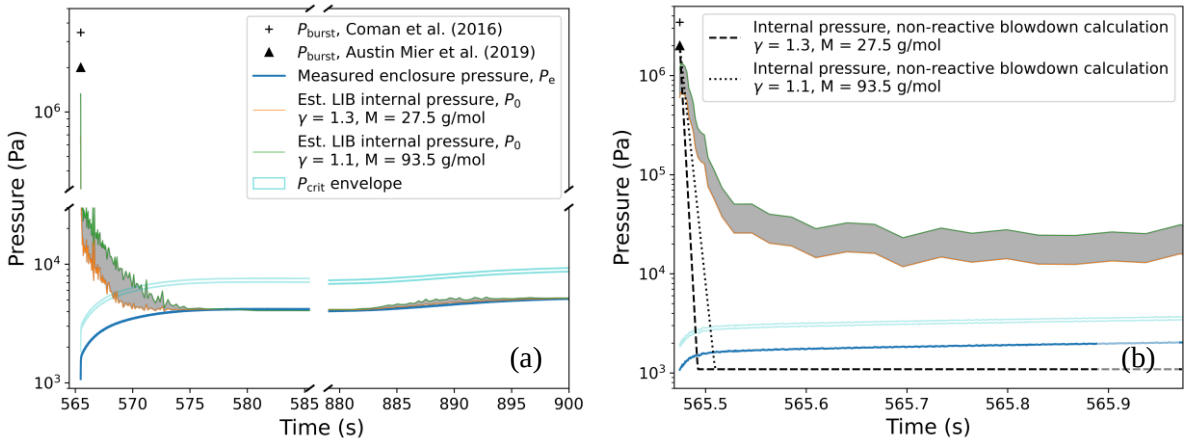

Figure 4: Measured and calculated pressures during a TR experiment with a heating rate of 20 °C/min. The shaded region represents the estimated LIB internal pressure (i.e., total pressure, P_0) range inferred from measured enclosure pressure P_e and the venting model.

Initial venting lasts for nearly 10 seconds. For comparison, the dashed and dotted lines in (b) represent calculations of the internal cell pressure for a blowdown of the gas available in the head space of the cell. In contrast to the experimental observation, the simulated blowdown would be completed within a few milliseconds. This indicates that gas generation takes place inside the cell after the vent opening due to continued electrolyte evaporation or decomposition, or reduced venting efficiency caused by multiphase flow. Other modelers have proposed that internal Darcy-Forchheimer flow further restricts the release of generated gases after the initial head space blowdown [9]. Additional pressure gain is observed in the TR region, remaining in a subsonic flow regime and producing 30% of the total moles.

5 Summary

Thermal runaway (TR) experiments were conducted using 18650 form-factor LIB cells to support the development of hazard and consequence models for LIB fires and explosions. In this study, LIBs were forced into TR by external heating and the effect of the heating rate was examined. During TR

propogation, not only can heat transfer between cells vary with configuration but also heat generated from igniton of the vented gases can vary the effective heating rates experienced by individual LIBs. Thus, measurements of the amount and types of gas released, plus their reactivity, is a key objective towards understanding the contributions of the vented gases to TR propagation. Direct measurements included LIB cell temperatures and gas pressures, and the vent gas was collected for composition analysis and further reactivity testing. In addition, the quantity of gas released was calculated from the internal temperature and pressure measurements.

Preliminary results indicate that the heating rate has a measurable effect on the cell temperature at the time of venting and TR, as well as on the quantity of gas released during each phase. These results suggest that experiments conducted at very low heating rates may not be indicative of TR of cells in real applications, where heating rates can be more than an order of magnitude higher than those used in typical TR experiments. Venting dynamics were further analyzed and internal cell pressures were inferred using a gas venting model, providing insight into the internal state of the cell and suggesting that internal gas generation occurs between the opening of the safety vent and the onset of TR.

Future work will include quantitative composition analysis of the vented gases, and reactivity analysis directly using the produced LIB vent gases or surrogate mixtures. The experimental database will be extended to further examine the effects of heating rate and establish procedures for TR testing of LIBs under conditions representative of typical TR scenarios.

References

[1] Q Wang, P Ping, X Zhao, G Chu, J Sun, and C Chen. Thermal runaway caused fire and explosion of lithium ion battery. J Power Sources. 2012; 208: p. 210-224.

[2] A O Said, C Lee, and S I Stoliarov. Experimental investigation of cascading failure in 18650 lithium ion cell arrays: Impact of cathode chemistry. J Power Sources. 2020; 446: p. 227347.

[3] P T Coman, S Rayman, and R E White. A lumped model of venting during thermal runaway in a cylindrical Lithium Cobalt Oxide lithium-ion cell. J Power Sources. 2016; 307: p. 56-62.

[4] F Austin Mier, M J Hargather, and S R Ferreira. Experimental Quantification of Vent Mechanism Flow Parameters in 18650 Format Lithium Ion Batteries. J Fluids Eng. 2019 April; 141.

[5] C R Bauwens, J Chaffee, and S Dorofeev. Effect of Ignition Location, Vent Size, and Obstacles on Vented Explosion Overpressures in Propane-Air Mixtures. Combust Sci Technol. 2010; 182: p. 1915-1932.

[6] A W Golubkov, D Fuchs, J Wagner, H Wiltsche, C Stangl, G Fauler, G Voitic, A Thaler, and V Hacker. Thermal-runaway experiments on consumer Li-ion batteries with metal-oxide and olivin-type cathodes. RSC Adv. 2014; 4(7): p. 3633-3642.

[7] A W Golubkov, S Scheikl, R Planteu, G Voitic, H Wiltsche, C Stangl, G Fauler, A Thaler, and V Hacker. Thermal runaway of commercial 18650 Li-ion batteries with LFP and NCA cathodes – impact of state of charge and overcharge. RSC Adv. 2015; 5(70): p. 57171-57186.

[8] A R Baird, E J Archibald, K C Marr, and O A Ezekoye. Explosion hazards from lithium-ion battery vent gas. J Power Sources. 2020; 446: p. 227257.

[9] J Kim, A Mallarapu, D P Finegan, and S Santhanagopalan. Modeling cell venting and gas-phase reactions in 18650 lithium ion batteries during thermal runaway. J Power Sources. 2021; 489: p. 229496.